ELSEVIER

Journal of Alloys and Compounds 225 (1995) 295–302

Journal of ALLOYS AND COMPOUNDS

Solid–liquid equilibria of neptunium(V) in carbonate solutions of different ionic strengths: II. Stability of the solid phases ☆

V. Neck [a], W. Runde [b], J.I. Kim [a,b]

[a] *Institut für Nukleare Entsorgungstechnik, Kernforschungszentrum Karlsruhe, D-76021 Karlsruhe, Germany*

[b] *Institut für Radiochemie, Technische Universität München, D-85747 Garching, Germany*

Abstract

The solid–liquid equilibria of Np(V) have been studied at 25 °C in 0.1–5 M $NaClO_4$ under 0.03% CO_2 in argon and in 5 M NaCl under 1.0% CO_2 in argon. The solid phases formed under given experimental conditions ($[CO_3^{2-}] = 10^{-8.0}$–$10^{-0.3}$ mol l^{-1}, pH = 6.8–10.5) have been characterized by X-ray diffraction analysis. At carbonate concentrations less than 10^{-3} mol l^{-1} and $[Na^+] = 0.1$–5 mol l^{-1}, $NaNpO_2CO_3$ was found to be the stable solid phase while, at higher carbonate concentrations and $[Na^+] \geq 1$ mol l^{-1}, the initial precipitate $NaNpO_2CO_3$ is slowly converted to $Na_3NpO_2(CO_3)_2$. The region of stability, i.e. the range of $NaClO_4$ and CO_3^{2-} concentration and pH, was determined for both solid phases. The Np(V) carbonate complexation constants and the solubility products of $NaNpO_2CO_3$ and $Na_3NpO_2(CO_3)_2$ were calculated at different $NaClO_4$ concentrations and in 5 M NaCl. The specific ion interaction theory was applied for the interpretation of the ionic strength effect and for the evaluation of thermodynamic constants at $I = 0$.

Keywords: Solubility; Sodium dioxoneptunyl carbonates; Carbonate complexation; Ionic strength

1. Introduction

The hydrolysis behaviour [1,2] and carbonate complexation reactions [3–9] of the NpO_2^+ ion have been studied systematically in $NaClO_4$ solution over a wide range of ionic strengths. In carbonate solution the chemistry of the NpO_2^+ ion is governed by the formation of the complexes $NpO_2CO_3^-$, $NpO_2(CO_3)_2^{3-}$ and $NpO_2(CO_3)_3^{5-}$. The Np(V) carbonate complexation constants have been determined by different approaches, e.g. solubility experiments [3–5], solvent extraction [6,7] and spectroscopic studies [3,8,9]. The reported results are in good agreement with one another as demonstrated recently by an intercomparison of these data with the specific ion interaction theory (SIT) formalism [3].

The present paper reports solid–liquid equilibrium experiments in carbonate-containing sodium salt solutions with particular interest in the solid phases obtained in equilibrium with the solutions investigated. A number of sodium neptunyl carbonates $Na_{2n-1}NpO_2(CO_3)_n \cdot xH_2O$ (with $n = 0.8$, 1, 2 and 2.5) have been reported by Volkov et al. [10–12] in the system Na_2CO_3–NpO_2^+–H_2O. Only $NaNpO_2CO_3$ and $Na_3NpO_2(CO_3)_2$ have been observed as solid phases in solubility studies published later [3–5,13,14]. Several workers [3–5] have determined the solubility product of $NaNpO_2CO_3$ in $NaClO_4$ solutions, but information on the solubility and stability of $Na_3NpO_2(CO_3)_2$ is rather poor. Simakin [13] reported solubility data in 3 M $NaNO_3$ at pH 12 and $[CO_3^{2-}] = 0.2$–1 mol l^{-1} without evaluating the solubility product of $Na_3NpO_2(CO_3)_2$ and Grenthe et al. [5] calculated a value of $\log K'_{sp} = -12.44$ from only one solubility value at $[CO_3^{2-}] = 0.1$ mol l^{-1} in 3 M $NaClO_4$.

The present study is concentrated on the determination of solubility products of $NaNpO_2CO_3$ and $Na_3NpO_2(CO_3)_2$ at different ionic strengths in order to evaluate the conditions under which these sodium neptunyl carbonates are formed as thermodynamically stable equilibrium solid phases. Experiments were performed in $NaClO_4$ solution, because of the non-complexing properties of the perchlorate ion, and also in concentrated NaCl solution, which is an interesting system with regard to nuclear waste storage in an underground salt mine.

☆ Part I: [3].

2. Experimental

2.1. Solubility experiment

The solid–liquid phase equilibrium studies have been performed at 25 °C in thermostatted 100 ml vessels filled with a gas mixture of 0.03% or 1.0% CO_2 in argon. The experiment was started with about 50 ml of $HClO_4$–$NaClO_4$ or HCl–NaCl solutions (pH about 3; $[NaClO_4]=0.1$, 1.0, 3.0 and 5.0 mol l^{-1}; $[NaCl]=5.0$ mol l^{-1}) containing about 50 mg of purified $^{237}Np(V)$. By adding $NaHCO_3$–$NaClO_4$ or $NaHCO_3$–NaCl solutions, the pH of each solution was increased to 8.0–8.5 and the NpO_2^+ ion precipitated. The thus-formed white precipitate ($NaNpO_2CO_3 \cdot xH_2O$) was left in contact with solution for several days. The chemical state of the initial precipitate $NaNpO_2CO_3$ was confirmed by X-ray powder diffraction analysis. During the equilibrium study, the pH was varied in the range 6.8–10.5 by adding $HClO_4$–$NaClO_4$ or $NaHCO_3$–$NaClO_4$ solution (or the corresponding chloride solution), while the Na^+ concentration was kept constant at the desired ionic strength. The water-saturated CO_2–Ar gas mixture, containing 0.03% CO_2 (0.1–5 M $NaClO_4$ solution) or 1.0% CO_2 (5 M NaCl), was passed through each solution for several days until the pH and the Np concentration remain constant, i.e. solid–liquid equilibrium state. The solubility curves were measured by increasing and by decreasing the carbonate concentration, i.e. from oversaturation and undersaturation.

After filtration (Sartorius membrane filters; pore size, 220 nm), the equilibrium concentration of Np(V) was measured radiometrically with a Beckman LS 6800 liquid scintillation counter, discriminating the β activity of the daughter nuclide ^{233}Pa from the α radiation of ^{237}Np. The oxidation state Np(V) in the starting solution ($[Np] \approx 2 \times 10^{-3}$ mol l^{-1}; pH about 3) was confirmed by absorption spectroscopy in the visible–near-IR region.

The conversion of white $NaNpO_2CO_3$ to grey–green $Na_3NpO_2(CO_3)_2$, which has been observed at $[CO_3^{2-}] > 10^{-2}$ mol l^{-1} and $[Na^+] \geq 1$ mol l^{-1}, was monitored by measuring the decrease in the Np(V) concentration during the time of solid-phase conversion. Both precipitates were identified by X-ray powder diffraction analysis.

2.2. Determination of pH and concentrations of H^+ and CO_3^{2-}

The present experiments have been performed under constant CO_2 partial pressures of $10^{-3.52}$ or $10^{-2.0}$ atm and the CO_3^{2-} concentration was calculated from the relation to the measured H^+ concentration. A combination glass electrode (Ross, Orion Co.), calibrated against $[H^+]$, $[OH^-]$ and pH buffer standards (pH 1–13; Merck Co.), was used for the pH measurement. In the case of pH measurement in $NaClO_4$ solutions, the original junction electrolyte (3 M KCl) was replaced by 3 M NaCl to avoid precipitation of $KClO_4$. Because of the salt effect on the liquid junction potential, the observed pH value pH_{exp} was shifted from the H^+ ion activity (pH equals $-\log(H^+)$) at the value $\Delta(pH)$, which varied with the junction solution and the salt concentration of the investigated solution. The difference is given by

$$pH = pH_{exp} + \Delta(pH) = -(\log[H^+] + \log \gamma_{H^+}) \quad (1)$$

The relations between pH_{exp} and analytical H^+ and OH^- concentrations, given by

$$\log[H^+] = -pH_{exp} - [\Delta(pH) + \log \gamma_{H^+}] \quad (2)$$

$$\log[OH^-] = pH_{exp} + \log K'_w + [\Delta(pH) + \log \gamma_{H^+}] \quad (3)$$

have been determined experimentally in each solution by measuring pH_{exp} in $NaClO_4$ and NaCl solutions containing $HClO_4$ (or HCl) (0.001–0.1 mol l^{-1}) and NaOH respectively. With the experimental values ($\log[H^+] + pH_{exp}$) and ($\log[OH^-] - pH_{exp}$), the apparent ion product of water is given by

$$\log K'_w = \log([H^+][OH^-])$$

$$= (\log[H^+] + pH_{exp}) + (\log[OH^-] - pH_{exp}) \quad (4)$$

The obtained values of $\log K'_w$ are in good agreement with generally accepted literature values [15] (Table 1). The $\Delta(pH)$ values also shown in Table 1 are estimated from Eqs. (2) and (3) by assuming that $\gamma_{H^+} \approx \gamma_{\pm}(H^+, OH^-)$. The mean activity coefficient of H^+ and OH^- ions, given by $\gamma_{\pm}(H^+, OH^-) = (a_w K_w / K'_w)^{1/2}$, is derived from the activity a_w of water [16,17] and the thermodynamic ion product of water ($\log K_w = -13.997$ [15]).

The CO_3^{2-} concentration is calculated from Eq. (5) or Eq. (6). The equilibrium constants, namely the Henry constant K'_H and the H_2CO_3 dissociation constants K'_1 and K'_2, are determined by potentiometric titration in each solution as integrated parameters K^* or $K' = K'_H K'_1 K'_2$:

$$\log[CO_3^{2-}] = \log K^* + \log[p(CO_2)] + 2\, pH_{exp} \quad (5)$$

$$\log[CO_3^{2-}] = \log K' + \log[p(CO_2)] - 2 \log[H^+] \quad (6)$$

The experimental values of $\log K^*$ and $\log K'$ are summarized in Table 1.

3. Results and discussion

3.1. Characterization of the equilibrium solid phases

The solid phases obtained in equilibrium with $NaClO_4$ and NaCl solutions under $10^{-3.52}$ and $10^{-2.0}$ atm CO_2 partial pressure have been characterized by X-ray pow-

Table 1
Ion product of water, observed pH shift and integrated H_2CO_3 dissociation constants (cf. Eqs. (5) and (6)) at 25 °C

I (mol l^{-1})	log K'_w	Δ(pH)	log K^*	log K'
$NaClO_4$				
0.1	−13.79±0.03 (−13.78) [a]	0.014±0.02 [b]	−17.78±0.03 [b]	−17.56±0.09
1.0	−13.81±0.04 (−13.80) [a]	0.33±0.02 [b]	−17.02±0.03 [b]	−17.47±0.10
3.0	−14.21±0.07 (−14.20) [a]	0.64±0.02 [b]	−16.54±0.02 [b]	−17.99±0.12
5.0	−14.90±0.06	0.86±0.04 [b]	−16.36±0.02 [b]	−18.88±0.08
NaCl				
5.0	−14.60±0.04	0.75±0.03 [c]	−16.28±0.04 [c]	−18.14±0.11

[a] [15].
[b] Liquid junction; 3 M NaCl.
[c] Liquid junction; 3 M KCl.

Table 2
Comparison of the X-ray patterns of the solid phases obtained in the present work and published by Volkov et al. [10,12]

$NaNpO_2CO_3 \cdot xH_2O$, this work		$NaNpO_2CO_3 \cdot 3.5H_2O$ [10]		$Na_3NpO_2(CO_3)_2 \cdot xH_2O$, this work		$Na_3NpO_2(CO_3)_2 \cdot xH_2O$ [12]	
d (pm)	Relative intensity (%)	d (pm)	Relative intensity (%)	d (pm)	Relative intensity (%)	d (pm)	Relative intensity (%)
985.9	100	987.0	100	606.9	20	607.0	21
492.4	80	491.5	80	578.2	20	575.0	25
441.1	40	440.7	30	439.8	100	439.1	100
435.0	50	435.0	30	427.1	<10	429.0	5
423.7	80	423.1	60	400.1	40	399.7	29
362.1	40	361.4	30	311.1	10	311.2	6
350.1	10	350.4	10	299.2	10	299.4	10
344.6	10	343.0	10	292.2	<10	291.4	10
328.5	20	327.5	10	281.7	10	280.4	6
320.3	70	319.5	80			271.3	4
292.1	50	291.4	30	253.7	40	253.4	50
290.1	40	289.1	30			233.6	3
251.8	10	251.7	10	219.8	30	219.4	38
244.7	40	244.0	30			214.0	4
238.7	10	237.2	5	209.5	10	210.4	4
236.3	10	235.2	10	199.1	10	200.0	7
220.8	<10	220.4	5			196.8	5
217.1	30	216.8	10	194.9	10	194.3	7
211.9	50	211.5	60			190.4	7

der diffraction. Typical results are shown in Table 2 in comparison with X-ray powder diffraction data published by Volkov et al. [10,12]. The diffraction data of the white precipitate produced at pH 8–8.5 are closely in agreement with the X-ray patterns reported for $NaNpO_2CO_3 \cdot 3.5H_2O$ [10]. The same solid phase was found by Maya [4] in 1.0 M $NaClO_4$ and by Grenthe et al. [5] in 3.0 M $NaClO_4$. The grey–green solid phase obtained by the conversion of $NaNpO_2CO_3$ at high carbonate concentrations in 1 M, 3 M and 5 M $NaClO_4$ and in 5 M NaCl shows X-ray patterns consistent with the data reported for $Na_3NpO_2(CO_3)_2 \cdot xH_2O$ [12]. Volkov et al. [10–12] described the colours of these sodium neptunyl carbonates as white and blue–green respectively. The formation of $NaNpO_2CO_3$ and $Na_3NpO_2(CO_3)_2$ as equilibrium solid phases is further confirmed by the dependence of the solubility data on Na^+ and CO_3^{2-} concentration (see below).

3.2. Solubility of $NaNpO_2CO_3$ and $Na_3NpO_2(CO_3)_2$

In carbonate-containing $NaClO_4$ solution, the concentration of the NpO_2^+ ion is related to the solubility products of either $NaNpO_2CO_3$ ($^{I}K'_{sp}$) or $Na_3NpO_2(CO_3)_2$ ($^{II}K'_{sp}$) by

$$^{I}K'_{sp} = [Na^+][NpO_2^+][CO_3^{2-}] \quad (7)$$

and

$$^{II}K'_{sp} = [Na^+]^3[NpO_2^+][CO_3^{2-}]^2 \quad (8)$$

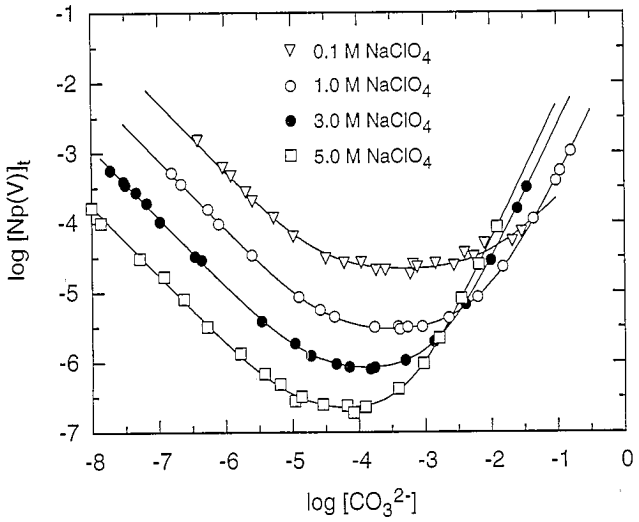

Fig. 1. Solubility of $NaNpO_2CO_3$ as a function of the CO_3^{2-} concentration in 0.1–5 M $NaClO_4$ ($p(CO_2)=10^{-3.52}$ atm) at 25 °C.

Table 3
Solubility products of $NaNpO_2CO_3$ and Np(V) carbonate complexation constants in 0.1–5 M $NaClO_4$ at 25 °C

I (mol l^{-1})	log K'_{sp}	log β'_1	log β'_2	log β'_3
0.1	−10.28±0.04	4.58±0.04	6.60±0.04	(<6.8)
1.0	−10.10±0.03	4.50±0.04	6.96±0.06	8.67±0.03
3.0	−10.45±0.04	4.76±0.04	7.69±0.07	10.30±0.09
5.0	−11.06±0.06	5.00±0.05	8.29±0.09	11.47±0.08

At pH<10, where hydrolysis reactions are negligible [1,2], Np(V) complexation reactions are restricted to the formation of the carbonate complexes $NpO_2CO_3^-$, $NpO_2(CO_3)_2^{3-}$ and $NpO_2(CO_3)_3^{5-}$ [3–9]. The formation constants β'_n at particular ionic strength are given by

$$\beta'_n = \frac{[NpO_2(CO_3)_n^{1-2n}]}{[NpO_2^+][CO_3^{2-}]^n} \quad (9)$$

With $NaNpO_2CO_3$ as the equilibrium solid phase the total concentration of aqueous Np(V) species is thus given by

$$[Np(V)]_t = [NpO_2^+] + \sum[NpO_2(CO_3)_n^{1-2n}] = \frac{{}^{I}K'_{sp}}{[Na^+][CO_3^{2-}]}\left(1+\sum\beta'_n[CO_3^{2-}]^n\right) \quad (10)$$

and in equilibrium with solid $Na_3NpO_2(CO_3)_2$ by

$$[Np(V)]_t = \frac{{}^{II}K'_{sp}}{[Na^+]^3[CO_3^{2-}]^2}\left(1+\sum\beta'_n[CO_3^{2-}]^n\right) \quad (11)$$

Fig. 1 shows the experimental solubility data in 0.1–5 M $NaClO_4$ obtained with the initial precipitate $NaNpO_2CO_3$. As expected according to Eqs. (7) and (10), at low carbonate concentrations, $\log[Np(V)]_t$ decreases linearily with a slope of −1 in the plot vs. $\log[CO_3^{2-}]$, and increasing the Na^+ concentration in a series of 0.1–5 M $NaClO_4$ causes lower solubilities. At higher carbonate concentrations the formation of Np(V) carbonate complexes, which has been confirmed by spectroscopic studies [3,8,9] becomes evident from the increase in the solubility curves. The solubility product of $NaNpO_2CO_3$ and the formation constants of the Np(V) carbonate complexes have been calculated from the solubility data in 0.1–5 M $NaClO_4$ by non-linear least-squares analysis. The results are summarized in Table 3.

In 0.1 M $NaClO_4$ solution, $NaNpO_2CO_3$ was found to be the stable solid phase over the whole CO_3^{2-} concentration range. In 1 M $NaClO_4$ the solubility experiment was continued up to pH 10.45 ($[CO_3^{2-}]=0.5$ mol l^{-1}) where, owing to the experimental conditions (50 mg ^{237}Np or less used for the experiment), $NaNpO_2CO_3$ was completely dissolved as aqueous Np(V) carbonate species. After several weeks, grey-green $Na_3NpO_2(CO_3)_2$ started to precipitate from the clear solution and the Np concentration decreased from $10^{-2.7}$ to $10^{-3.7}$ mol l^{-1}. In 3 M and 5 M $NaClO_4$, and in 5 M NaCl, the initial solid phase $NaNpO_2CO_3$ had been converted to less soluble $Na_3NpO_2(CO_3)_2$ at considerably lower carbonate concentrations ($[CO_3^{2-}]=10^{-1.9}$–$10^{-1.5}$ mol l^{-1}). During the time of solid-phase conversion, which takes place over 10 days, the Np(V) concentration in solution decreased significantly, i.e. by more than an order of magnitude at constant H^+ and CO_3^{2-} concentrations (Fig. 2).

After solid-phase conversion the solid–liquid equilibrium experiment was continued with $Na_3NpO_2(CO_3)_2$ as a thermodynamically stable solid phase in the region of high carbonate concentrations. The results are shown in Fig. 3, which provides further evidence for the chemical state of the solid phases $NaNpO_2CO_3$ and $Na_3NpO_2(CO_3)_2$ involved in the present experiment. As demonstrated by absorption spectroscopy, the third Np(V) carbonate complex $NpO_2(CO_3)_3^{5-}$ becomes the predominant species at CO_3^{2-} concentrations above 10^{-2} mol l^{-1}. With $NaNpO_2CO_3$, a metastable solid phase under these conditions, the solubility curves in Fig. 3 increase with a slope of +2 in the high carbonate concentration range as expected according to

$$\log[Np(V)]_t \approx \log[NpO_2(CO_3)_3^{5-}] = \log\left(\frac{{}^{I}K'_{sp}\beta'_3}{[Na^+]}\right) + 2\log[CO_3^{2-}] \quad (12)$$

In contradiction to this, the solubility curves obtained in equilibrium with $Na_3NpO_2(CO_3)_2$ increase with a slope of +1 at $[CO_3^{2-}]>10^{-2}$ mol l^{-1}:

$$\log[Np(V)]_t \approx \log[NpO_2(CO_3)_3^{5-}] = \log\left(\frac{{}^{II}K'_{sp}\beta'_3}{[Na^+]^3}\right) + \log[CO_3^{2-}] \quad (13)$$

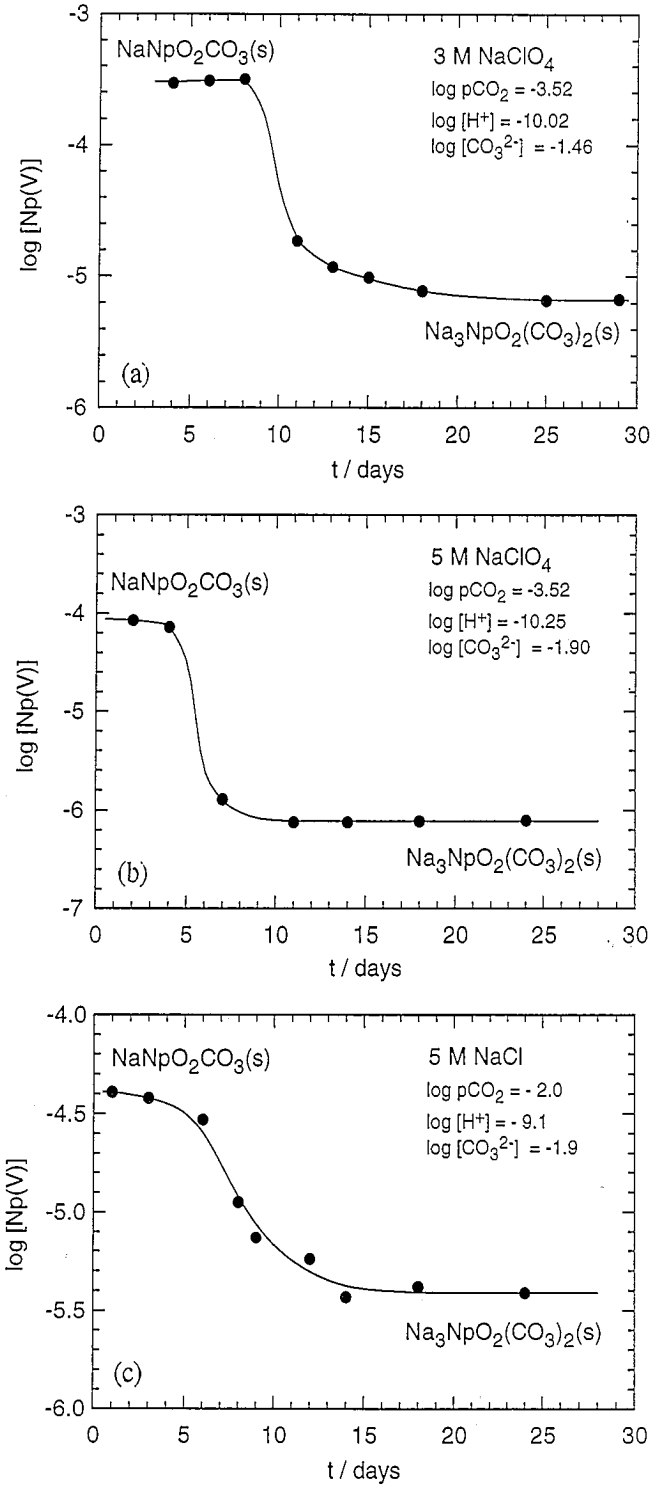

Fig. 2. Decrease in Np(V) concentration during the time of solid phase conversion in (a) 3 M $NaClO_4$, (b) 5 M $NaClO_4$ and (c) 5 M NaCl.

When the carbonate concentration was varied to lower values, where $NaNpO_2CO_3$ is thermodynamically stable, i.e. its solubility was lowered compared with the values of $Na_3NpO_2(CO_3)_2$, the solubility data correspond to the curve obtained in the beginning of the experiment with $NaNpO_2CO_3$ as the initial solid phase.

With the carbonate complexation constants calculated from the solubility data of $NaNpO_2CO_3$ (Table 3), the solubility products of $Na_3NpO_2(CO_3)_2$ were evaluated by least-squares analysis from the experimental data in the high carbonate concentration range. The solubility data of $Na_3NpO_2(CO_3)_2$ in the low carbonate concentration range (broken curves in Fig. 3) can thus be calculated from Eq. (11).

The solubility products of $NaNpO_2CO_3$ and $Na_3NpO_2(CO_3)_2$ determined in 0.1–5 M $NaClO_4$ and in 5 M NaCl are summarized in Table 4, together with the literature values known hitherto. The $\log[{}^{I}K'_{sp}(NaNpO_2CO_3)]$ values published by Maya [4] for 1 M $NaClO_4$ and by Grenthe et al. [5] for 3 M $NaClO_4$ agree very well with the present values. The $\log[{}^{II}K'_{sp}(Na_3NpO_2(CO_3)_2)]$ value determined by Grenthe et al. [5] from only one solubility datum in 3 M $NaClO_4$ is in good agreement with the present result.

In 5 M NaCl, where 90.4% of the NpO_2^+ ion form complexes with the chloride ion [18], the solubility of Np(V) is significantly increased compared with that in 5 M $NaClO_4$. Therefore the evaluation of solubility products and carbonate complexation constants from Eqs. (7)–(11) leads to the apparent values K^*_{sp} and β^*_n, including Np(V) chloride complexation. In 5 M NaCl the apparent neptunyl ion concentration is given by

$$[NpO_2^+]^* = [NpO_2^+] + [NpO_2Cl^0] + [NpO_2Cl_2^-]$$

$$= [NpO_2^+]\left(1 + \sum \beta'_x [Cl^-]^x\right) \quad (14)$$

To obtain the real K'_{sp} values shown in Table 4, the apparent solubility products K^*_{sp} have been corrected according to

$$K'_{sp} = K^*_{sp} \Big/ \left(1 + \sum \beta'_x [Cl^-]^x\right) \quad (15)$$

with the Np(V) chloride complexation constants $\beta'_1 = 0.90 \pm 0.05$ and $\beta'_2 = 0.20 \pm 0.02$ [18].

3.3. Ionic strength effect and thermodynamic stability of $NaNpO_2CO_3$ and $Na_3NpO_2(CO_3)_2$

The question of which of the neptunyl carbonates is the stable equilibrium solid phase responsible for the solubility of Np(V) under given conditions (ionic strength, carbonate concentration and pH) requires the determination of the thermodynamic solubility products at $I = 0$ and the interpretation of the ionic strength effect. The SIT, which is based on the earlier work of Scatchard [19] and later refined by Ciavatta [20] for its broad application, has been used by many workers to describe the ionic strength dependence of solution equilibria [1,5,8,9]. The formation of Np(V) carbonate

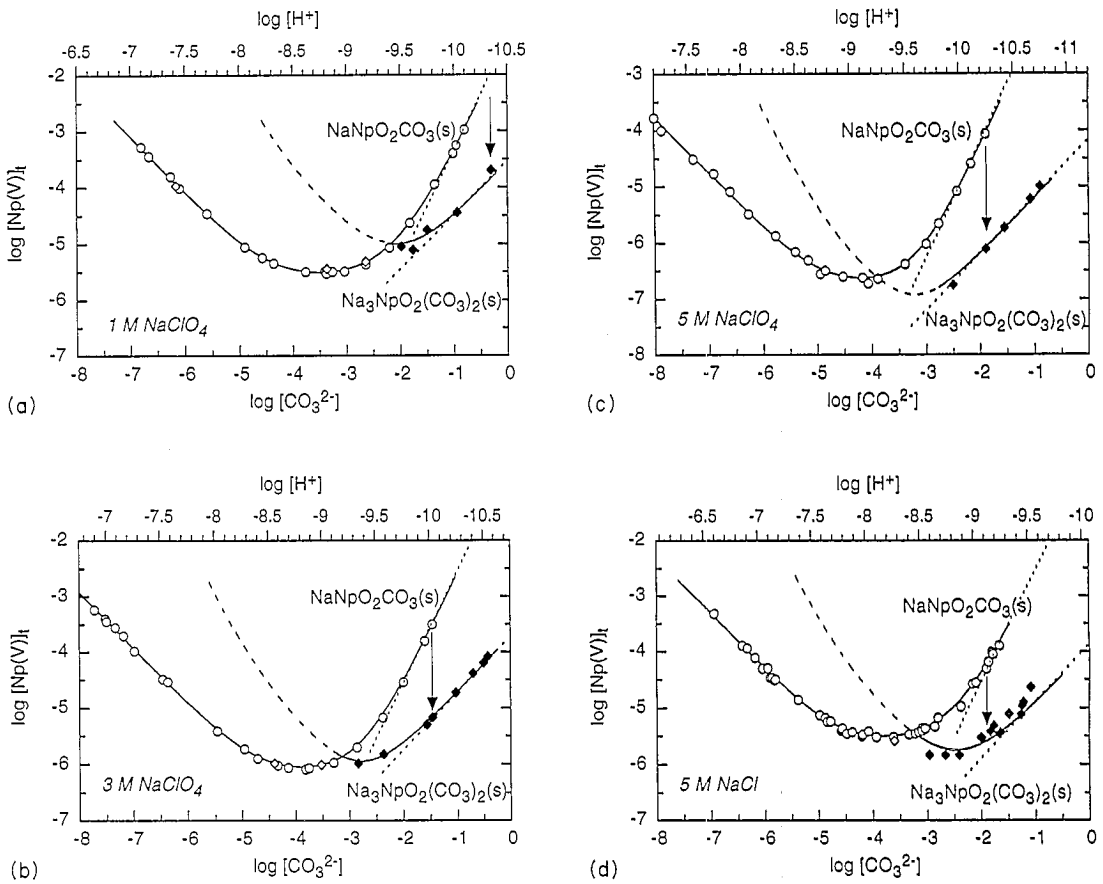

Fig. 3. Solubility of $NaNpO_2CO_3$ and $Na_3NpO_2(CO_3)_2$ at 25 °C as a function of the H^+ and CO_3^{2-} concentration: (a) in 1 M $NaClO_4$ under $p(CO_2)=10^{-3.52}$ atm; (b) in 3 M $NaClO_4$ under $p(CO_2)=10^{-3.52}$ atm; (c) in 5 M $NaClO_4$ under $p(CO_2)=10^{-3.52}$ atm; (d) in 5 M NaCl under $p(CO_2)=10^{-2.00}$ atm.

Table 4
Solubility products of $NaNpO_2CO_3$ and $Na_3NpO_2(CO_3)_2$ at 25 °C

I (mol l^{-1})	log ${}^{I}K'_{sp}(NaNpO_2CO_3)$	log ${}^{II}K'_{sp}(Na_3NpO_2(CO_3)_2)$
$NaClO_4$		
0.1	-10.28 ± 0.04	
1.0	-10.10 ± 0.03 (-10.14 ± 0.04 [4])	-12.23 ± 0.15
3.0	-10.45 ± 0.04 (-10.56 [5])	-12.59 ± 0.10 (-12.44 [5])
5.0	-11.06 ± 0.06	-13.57 ± 0.11
NaCl		
5.0	-9.61 ± 0.11 (log ${}^{I}K^*_{sp}$)	-11.46 ± 0.23 (log ${}^{II}K^*_{sp}$)
	-10.63 ± 0.11 (log ${}^{I}K'_{sp}$)	-12.48 ± 0.23 (log ${}^{II}K'_{sp}$)

complexes has been described successfully by the SIT up to an $NaClO_4$ concentration of 3 mol l^{-1} [3]. According to this semi-empirical approach, ionic activity coefficients γ_i in a given medium are estimated from

$$\log \gamma_i = -z_i^2 D + \epsilon_{ij} I_m \quad (16)$$

where z_i is the ionic charge, D is the Debye–Hückel term: $0.5107\ I_m^{1/2}/(1+B\dot{a}I_m^{1/2})$, with $B\dot{a}=1.5$ as suggested by Scatchard, I_m is the ionic strength (molal concentration scale), and ϵ_{ij} is the ion–ion interaction parameter for each pair of ions involved in the system.

The thermodynamic constant K^0 is thus related to K' at given ionic strength by

$$\log K' - \Delta z^2 D = \log K^0 - \Delta\epsilon I_m \quad (17)$$

with $\Delta z^2 = \Sigma z_i^2(\text{products}) - \Sigma z_i^2(\text{educts})$ and $\Delta\epsilon = \Sigma\epsilon_{ij}(\text{products}) - \Sigma\epsilon_{ij}(\text{educts})$.

After conversion in the molal concentration scale, the experimental log K'_{sp} in Table 4 are plotted according to Eq. (17) as shown in Fig. 4, and the interaction parameters $\Delta\epsilon$ and the thermodynamic constants at $I=0$ are calculated by linear least-squares regression

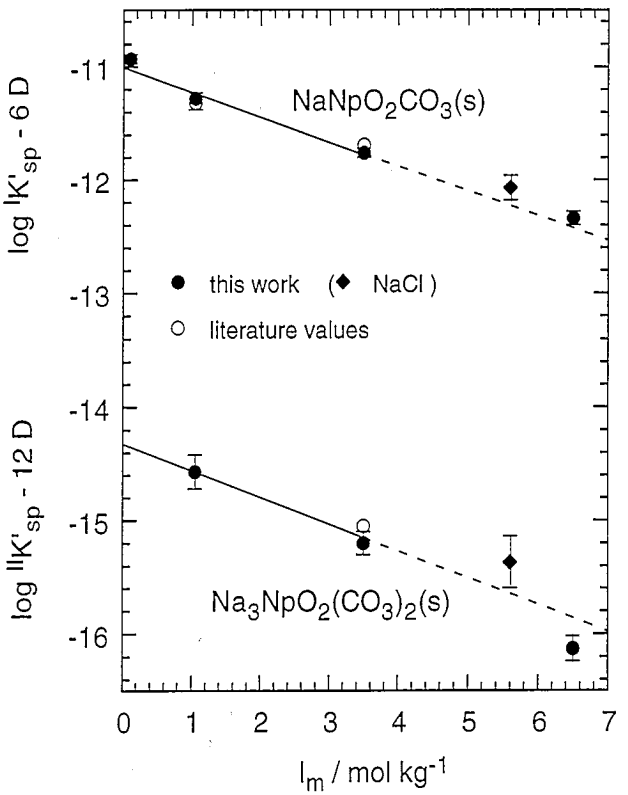

Fig. 4. Determination of the thermodynamic solubility products of $NaNpO_2CO_3$ and $Na_3NpO_2(CO_3)_2$ according to the SIT formalism.

Table 5
The specific ion interaction theory parameters describing the ionic strength dependence of the solubility products of $NaNpO_2CO_3$ and $Na_3NpO_2(CO_3)_2$ at 25 °C

	Δz^2	$\Delta\epsilon$ (I_m = 0.1–3.5)	log K^0_{sp}
$NaNpO_2CO_3$	+6	+0.22±0.03	−11.00±0.07
$Na_3NpO_2(CO_3)_2$	+12	+0.24±0.08	−14.32±0.15

using the data up to $I_m = 3.5$ mol kg^{-1} (3.0 M $NaClO_4$), for which the validity of the SIT is known to be restricted. In the present case, however, the linear extrapolation to higher ionic strength (broken curves in Fig. 4) does not deviate significantly from the experimental data in 5.0 M $NaClO_4$ (6.5 mol kg^{-1}), and even the data in 5.0 M NaCl (5.6 mol kg^{-1}) are close to the extrapolated lines. The calculated parameters of Eq. (17) are summarized in Table 5. the SIT parameters describing the formation of the soluble Np(V) carbonate species have been discussed recently [3].

Since the data for the solubility product of $Na_3NpO_2(CO_3)_2$ show relatively large uncertainties and extrapolation to $I = 0$ is made without experimental data at $I < 1$ mol kg^{-1}, the calculated constant of log $^{II}K^0_{sp} = -14.44 \pm 0.23$ is further examined by the relations between K^0_{sp} and K'_{sp} values, which are correlated to each other by the activity coefficients of the ions involved:

$$^{I}K^0_{sp} = {}^{I}K'_{sp}\gamma(Na^+)\gamma(NpO_2^+)\gamma(CO_3^{2-}) \quad (18)$$

$$^{II}K^0_{sp} = {}^{II}K'_{sp}\gamma^3(Na^+)\gamma(NpO_2^+)\gamma^2(CO_3^{2-}) \quad (19)$$

Combining Eqs. (18) and (19), the thermodynamic solubility product of $Na_3NpO_2(CO_3)_2$ is given by

$$\log {}^{II}K^0_{sp} = 2(\log {}^{I}K^0_{sp} - \log {}^{I}K'_{sp}) + \log {}^{II}K'_{sp} - \log\left(\frac{\gamma(NpO_2^+)}{\gamma(Na^+)}\right) \quad (20)$$

The experimental values log $^{I}K'_{sp}$ and log $^{II}K'_{sp}$ are shown in Table 4; log $^{I}K^0_{sp}$ was evaluated with sufficient accuracy by the SIT formalism as shown above; the ratios of the activity coefficients $\gamma(NpO_2^+)$ and $\gamma(Na^+)$ have been determined recently in $NaClO_4$ and NaCl solutions up to $I = 5$ mol l^{-1} [18] and are given in Table 6. The thermodynamic solubility product of $Na_3NpO_2(CO_3)_2$ calculated in this way (log $^{II}K^0_{sp} = -14.44 \pm 0.23$) is in good agreement with the extrapolated value obtained by the SIT formalism (-14.32 ± 0.15).

Knowing the solubility products over the total $NaClO_4$ concentration range, it is possible to calculate whether the solubility of Np(V) is controlled by Eq. (10) or by Eq. (11), i.e. whether $NaNpO_2CO_3$ or $Na_3NpO_2(CO_3)_2$ is a stable solid phase under given conditions. Figure 5 shows the stability regions of the Np(V) solid phases

Table 6
The ratios log[$\gamma(NpO_2^+)/\gamma(Na^+)$] and log $^{II}K^0_{sp}$ values in $NaClO_4$ and NaCl solutions

	log[$\gamma(NpO_2^+)/\gamma(Na^+)$]	log $^{II}K^0_{sp}$
1 M $NaClO_4$	0.17	−14.20±0.18
3 M $NaClO_4$	0.62	−14.31±0.15
5 M $NaClO_4$	1.27	−14.72±0.18
5 M NaCl	0.30	−14.54±0.33
		Mean value −14.44±0.23

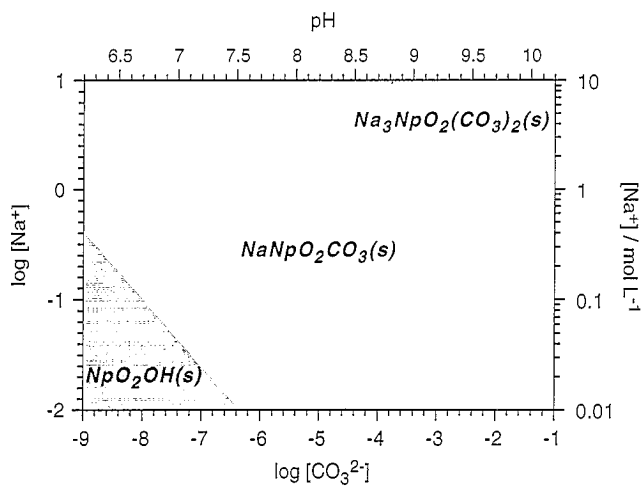

Fig. 5. Stability regions of the Np(V) solid phases in the system $NaClO_4$–CO_3^{2-} ($p(CO_2) = 10^{-3.52}$ atm) at 25 °C.

in the $NaClO_4$–carbonate system under atmospheric CO_2 partial pressure at 25 °C. The higher the Na^+ and carbonate concentrations, the more $Na_3NpO_2(CO_3)_2$ becomes a stable solid phase. At $[Na^+] \geq 0.1$ mol l^{-1}, only $NaNpO_2CO_3$ should be stable. This result is confirmed by the experiment in 0.1 M $NaClO_4$. Volkov et al. [10] observed the precipitation of $NaNpO_2CO_3$ in Na_2CO_3 solutions up to 0.1 mol l^{-1} and the precipitation of $Na_3NpO_2(CO_3)_2$ at Na_2CO_3 concentrations greater than 0.3 mol l^{-1}, which are both predicted by Fig. 5. At very low Na^+ and CO_3^{2-} concentrations, of course, neither $NaNpO_2CO_3$ nor $Na_3NpO_2(CO_3)_2$ (but neptunyl hydroxide NpO_2OH) is expected as an equilibrium solid phase. On the basis of our previous studies on the solubility of amorphous NpO_2OH (log $K^0_{sp} = (NpO_2^+)(OH^-) = -8.76 \pm 0.05$; $\Delta\epsilon = 0.23 \pm 0.04$ [2]), and with the correlation between OH^- and CO_3^{2-} concentration at constant $p(CO_2)$ given by Eqs. (4)–(6), this region is also calculated as illustrated in Fig. 5.

4. Conclusions

The present results enable us to predict the stable Np(V) solid phase in $NaClO_4$ solutions of known ionic strength, pH and carbonate concentration and also to calculate the solubility limit, i.e. the concentration of aqueous Np(V) species, from the corresponding solubility product and the formation constants of the Np(V) hydrolysis species and carbonate complexes.

References

[1] Ch. Lierse, W. Treiber and J.I. Kim, *Radiochim. Acta, 38* (1985) 27.
[2] V. Neck, J.I. Kim and B. Kanellakopulos, *Radiochim. Acta, 56* (1992) 25.
[3] V. Neck, W. Runde, J.I. Kim and B. Kanellakopulos, *Radiochim. Acta, 65* (1994) 29.
[4] L. Maya, *Inorg. Chem., 22* (1983) 2093.
[5] I. Grenthe, P. Robouch and P. Vitorge, *J. Less-Common Met., 122* (1986) 225.
[6] G. Bidoglio, G. Tanet and A. Chatt, *Radiochim. Acta, 38* (1985) 21.
[7] Y. Inoue, O. Tochiyama, *Bull. Chem. Soc. Jpn., 58* (1985) 588.
[8] H. Nitsche, E.M. Standifer and R.J. Silva, *Lanth. Act. Res., 3* (1990) 203.
[9] C. Riglet, *Rapp. CEA-R-5535,* 1990 (Centre d'Etudes Nucléaires Fontenay aux Roses, France).
[10] Yu.F. Volkov, G.I. Visyashcheva and I.I. Kapshukov, *Sov. Radiochem., 19* (1977) 263.
[11] Yu.F. Vokov, G.I. Visyashcheva, S.V. Tomilin, V.I. Spiryakov, I.I. Kapshukov and A.G. Rykov, *Sov. Radiochem., 21* (1979) 583.
[12] Yu.F. Volkov, G.I. Visyashcheva, S.V. Tomilin, I.I. Kapshukov and A.G. Rykov, *Sov. Radiochem., 23* (1981) 191, 195.
[13] G.A. Simakin, *Sov. Radiochem., 19* (1977) 424.
[14] R.J. Lemire, G.D. Boyer and A.B. Campbell, *Radiochim. Acta, 61* (1993) 57.
[15] Ch.F. Baes, R.E. Mesmer, *The Hydrolysis of Cations,* Wiley, New York, 1976.
[16] Y. Marcus and A.S. Kertes, *Ion Exchange and Solvent Extraction of Metal Complexes,* Wiley, New York, 1969.
[17] J.H. Jones, *J. Phys. Chem., 51* (1947) 516.
[18] V. Neck, J.I. Kim and B. Kanellakopulos, *Ber. KfK 5301,* 1994 (Kernforschungszentrum Karlsruhe).
[19] G. Scatchard, *Chem. Rev., 19* (1936) 309.
[20] L. Ciavatta, *Ann. Chim. (Rome),* (1980) 551.